Korea-Australia Rheology Journal
Vol. 18, No. 3, September 2006 pp. 143-151

Numerical analysis of internal flow and mixing performance in polymer extruder I: single screw element

Naksoo Kim*, Hongbum Kim and Jaewook Lee[1]
Dept. of Mechanical Engineering, Sogang University,
[1]Dept. of Chemical and Biomolecular Engineering, Sogang University, 1, Sinsu-dong, Mapo-gu, Seoul 121-742, Korea
(Received June 6, 2006; final revision received August 28, 2006)

Abstract

We analyzed the non-Newtonian and non-isothermal flow in a single screw extruder system and investigated the mixing performance with respect to the screw speed and the screw pitch. The viscosity of polymer melt was described with Carreau-Yasuda model. The mixing performance was computed numerically by tracking the motions of particles in the screw element system. The extent of mixing was characterized in terms of the deformation rate, the residence time distribution, and the strain. The results revealed that the high screw speed reduces the residence time but increases the deformation rate while the small screw pitch increases the residence time. It is concluded that the high screw speed increases the dispersive mixing performance and the small screw pitch increases the distributive mixing performance.

Keywords : nano-composite, polymer extrusion process, single screw extruder, mixing performance, particle tracking, residence time distribution

1. Introduction

As a screw extrusion process is a continuous and thermally and mechanically uniform manufacturing method, it is applied for production of high molecular material to fabricate nano-composites. Excellent design of screw extruder and optimization of process conditions may enhance the efficiency of mixing performance of nano-scaled clay particles in polymer matrix. Despite the importance of design and analysis of polymer extrusion processes to manufacture nano-composites with uniformly distributed clay particles, the lack of researches on the screw extruders makes industry to design and to operate the process based on the experience rather than on the systematic knowledge. It is imperative that we analyze the flow characteristics of polymer melt in a screw extruder with proper numerical methods and obtain the data to be utilized in the actual processes.

Most numerical analyses on the screw extrusion process have been done with simplified geometries and with many assumptions due to the difficulties lying in modeling of complicated shape of screw extruders. Though we may grasp and investigate the basic tendencies about the polymer flow through modeling with approximate geometries and with many assumptions, it is not easy for us to understand the detailed flow characteristics of polymer melt in a screw extruder.

Griffith (1962) analyzed the fully developed flow of incompressible fluid in a single screw extruder with an assumption that the velocity and the temperature profiles are equal in infinite plane using power-law viscosity model. Fenner (1977) analyzed the flow in a screw extruder and the temperature development along the screw channel. Karwe and Jaluria (1990) solved thermal transfer of a non-Newtonian fluid with assumptions that the temperature distribution is known and adiabatic conditions are applied onto the screw surface. Sastrohartono *et al.* (1994) analyzed the flow in a screw extruder by using the marching scheme to describe the circulation flow in channel and then verified the results with experiments. Raman *et al.* (1996) extended the previous research and successfully analyzed the reverse flow due to back pressure. Kim and Kwon solved the three dimensional velocity fields in a single screw extruder using the finite element method and proposed the screw design to enhance the mixing performance. (Kim and Kwon, 1996a, 1996b)

Ghoreishy and Nouri (1999) carried out a numerical analysis of the high molecular fluid flow using the finite element method in the metering section and the die. They verified the numerical results with experiments. Syrjala (1999) carried out a research on the three dimensional fluid flow in the conveying section of single screw extruder using the marching scheme which contiguously solved the equation given in the perpendicular section to down channel. The validity of the methodology has been verified later

*Corresponding author: nskim@sogang.ac.kr

with experiment data (Syrjala, 2000). Kwag *et al.* (2001) performed researches on the three dimensional flow and the thermal analysis of non-Newtonian fluid in a single screw extruder using a commercial code, STAR-CD, based on the finite volume method. They overcame the limit of marching scheme (Syrjala, 1999; 2000) in analyzing the reverse flow due to back pressure.

Previous researches have the limit of accuracy because of using simplified models of screw extruders. Ahmad and Jean-Robert (2005) modeled a screw extruder without geometry approximation and carried out a three dimensional numerical analysis for the non-isothermal steady-state flows using the finite volume method. Ye *et al.* (2005) carried out a research about polymer extrusion processes with the finite element method using a 4-step fractional method.

So far, most researches have analyzed the polymer flow in single screw extruders with simplified modeling or assumption of contiguous quasi-steady states because of difficulty in describing analysis domain of screw extruder with dynamic boundary conditions. Assumption of quasi-steady states may yield to significant errors, because of that the convection effect is bigger than that of conduction in calculating the temperature filed. Especially, the error resulted from the assumption of quasi-steady states increases as the screw speed becomes fast enough that the influence of convection increases. The flow in a screw extruder is non-steady state since the flow channel varies with time due to the rotation of the screw element in a barrel. As the flow in a screw extruder is a dynamic boundary problem, we may improve the accuracy of numerical results by regarding the problem as a 3-D, non-steady state, and non-isothermal flow.

In this study, we modeled and analyzed sectional screw elements as detailed as possible to investigate the flow field and to understand the effect of processing parameters. Preliminary numerical results showed that the mixing performance varied with processing parameters and geometries. The final goal of this study is to establish a proper method of numerical analysis for screw extrusion processes.

2. Geometry and process parameters

2.1. Shape of screw extruder

A single screw extruder is modeled as shown in Fig. 1 to calculate the mixing performance with respect to the screw speed as a process parameter and the screw pitch length as a geometry parameter. The geometry of the screw element has been chosen as simple as possible to avoid manufacturing difficulties in the future experimental verification. Symbols and dimensions of geometric parameters used in modeling of analysis domain are shown in Fig. 2 and Table 1, respectively. Modeling method to analyze the dynamic boundary problem is illustrated in Fig. 3 and the detailed procedure of modeling is explained in section 2.4.

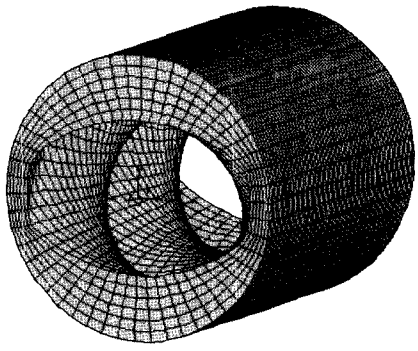

Fig. 1. Screw extruder analysis domain.

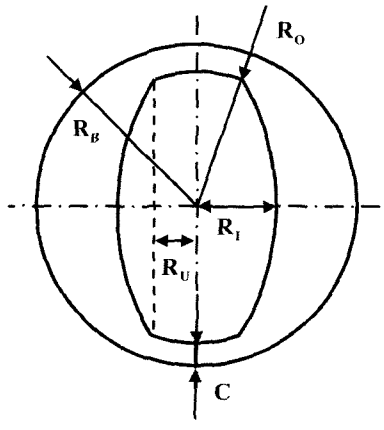

Fig. 2. Cross section of screw extruder.

Table 1. Dimensions of Screw extruder

R_B	R_O	R_I	R_U	C
13 mm	11 mm	7 mm	3 mm	2 mm

2.2. Assumptions for numerical modeling

It is proper to assume that the flow regime in a screw extruder is laminar, because Reynold's number of polymer melt is small enough due to its high viscosity. Product quality produced by extrusion processes is mainly determined in the metering section that conveys the polymer melt to be mixed efficiently under the constant temperature and pressure. Current analysis is focused to the metering section in a screw extruder to investigate the mixing performance. The designated domain is adequate for this study purpose. Namely this domain is reflected enough for the whole appearance of screw extruder. Even though an assumption that the barrel is fully filled with polymer melt is not true in actual industrial cases, it may be justified to investigate the flow characteristics of polymer melt and the relative mixing performance from the obtained numerical results.

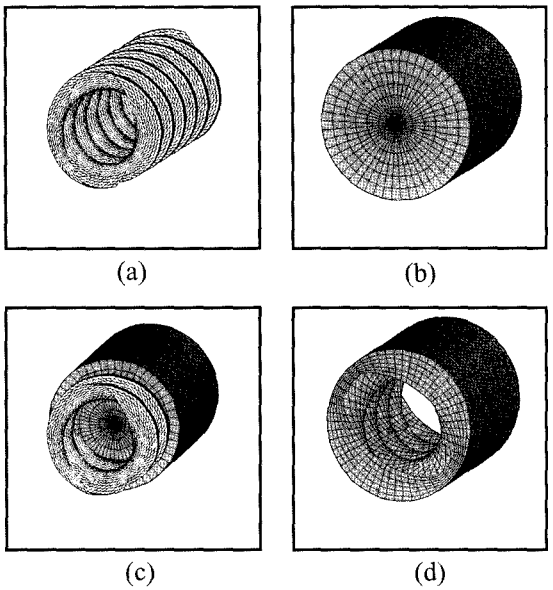

Fig. 3. Modeling procedure of analysis domain; (a) modeling of screw, (b) modeling of barrel cavity, (c) subtracting screw from barrel cavity, and (d) completed barrel cavity.

Assumptions used for the flow analysis of screw extruder are summarized as follows:

(1) The flow regime in screw extruder is laminar.
(2) The polymer melt is an incompressible fluid.
(3) The viscosity is modeled to a function of temperature and shear rate.
(4) Heat is generated due to the viscous dissipation of polymer melt.
(5) Thermal condition between the screw surface and the polymer melt is adiabatic.
(6) The no-slip condition is imposed onto the solid boundary.
(7) Density and specific heat are constant.
(8) The barrel is fully filled with polymer melt.
(9) The steady state flow of polymer melt is attained after the screw rotates enough revolutions. During each time step, the screw rotates by a given angle.

2.3. Boundary conditions

Based on the assumptions described in the previous section, the following boundary conditions to the flow problem in a screw extruder have been imposed:

(1) No-slip boundary condition is imposed on the solid surfaces of screw and barrel. In other words, the relative velocity of polymer melt faced with solid in each direction is zero.
(2) Barrel temperature is uniform overall as 200°C.
(3) Initial temperature of polymer melt at inlet is constant to 190°C and the temperature boundary condition at outlet is $dT/dz = 0$.
(4) Pressures at inlet and outlet are set to be zero.

2.4. Modeling procedure of analysis domain

Analysis domain is modeled according to the following procedures as illustrated in Fig. 3:

(1) Model the screw shape using I-DEAS as shown in Fig. 3(a) and transform the modeled screw surface to the shell mesh.
(2) Model the barrel cavity mesh in STAR-CD as shown in Fig. 3(b).
(3) Overlap the screw shell mesh and the fluid mesh in barrel cavity as shown in Fig. 3(c).
(4) Rotate the screw shell mesh according to the screw rotation speed and project the fluid mesh to the rotated screw shell mesh. After subtracting the screw mesh from the barrel cavity at each rotating angle, the completed cavities are ready for the calculation, as shown in Fig. 3(d). As a result, the same number of barrel cavities is modeled as the number of specified rotating angles.

3. Theory

3.1. Governing equations

Polymer melt is a non-Newtonian fluid. It experiences a non-steady, incompressible, and the laminar flow. To express the flow of polymer melt having these natures, the continuity and the momentum equations in Cartesian coordinate system are given as follows:

$$\frac{\partial \rho}{\partial t} + \frac{\partial}{\partial x_i}(\rho u_i) = s_m \tag{1}$$

$$\frac{\partial \rho u_i}{\partial t} + \frac{\partial}{\partial x_i}(\rho u_j u_i + \tau_{ij}) = -\frac{\partial p}{\partial x_i} + s_i \tag{2}$$

$$\frac{\partial \rho h_t}{\partial t} + \frac{\partial}{\partial x_i}(\rho h_t u_j + F_{h,j}) = \frac{\partial p}{\partial t} + u_j \frac{\partial p}{\partial x_j} + \tau_{ij}\frac{\partial u_i}{\partial x_j} + s_h - \sum_m H_m s_{c,m} \tag{3}$$

The source terms in equations (1) and (3) are discretized by the piso algorithm and the source term linearization in the commercial code, STAR-CD. The first term in equations (1) is zero since the density do not varies with time. The flux term is solved by the upwind scheme. Shear stress τ_{ij} is expressed by the following constitutive law.

$$\tau_{ij} = 2\mu s_{ij} - \frac{2}{3}\mu \frac{\partial u_k}{\partial x_k}\delta_{ij}, \tag{4}$$

where $s_{ij} = \frac{1}{2}\left(\frac{\partial u_i}{\partial x_j} + \frac{\partial u_j}{\partial x_i}\right)$.

3.2. Viscous model

The Carreau-Yasuda model is considered as a fluid viscous model. This model as functions of deformation rate

Table 2. Material properties of low density polyethylene

Viscosity model	
Power-law index, n	0.334
Power-law constant, K [Pa-s^n]	16,630
Reference temperature, T_{ref} [°C]	150
Temperature sensitivity, β [°C]	5260
Time constant, λ [s]	0.6247
Zero shear strain viscosity,	12,156
Physical properties	
Thermal conductivity,	0.21
Density, ρ [kg/m^3]	785
Heat capacity, C [j/kg°C]	2780

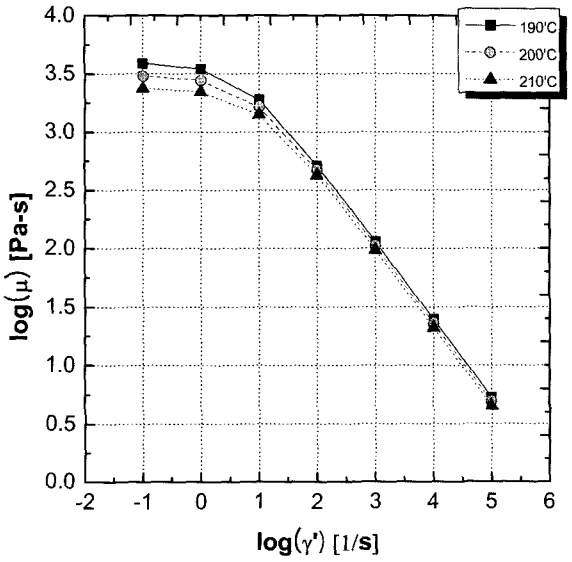

Fig. 4. Viscosity model used for low-density polyethylene.

and temperature is expressed by equation (5). It is transformed to a user subroutine to be called by STAR-CD.

$$\mu = \mu_0 \alpha [1 + (\lambda \alpha \dot{\gamma})]^{(n-1)} \tag{5}$$

In equations (5), α is a temperature shift factor and $\dot{\gamma}$ is the deformation rate and each of these is expressed as follows:

$$\alpha = \exp\left[\beta\left(\frac{1}{T} - \frac{1}{T_{ref}}\right)\right] \text{ and } \dot{\gamma} = \sqrt{\frac{1}{2}(s_{ij}s_{ij} - s_{ii}s_{jj})}.$$

The values used in the computation are listed in Table 2. The curves that express viscous equation (5) are shown in Fig. 4.

Whenever the shear rate is computed too high or too low at initial stages of non-steady state calculation using the above viscous models, the convergence speed may become slow or even the numerical result may diverge. As the shape of analysis domain changes due to the rotation of screws, the unrealistic values of viscosity may be calculated due to the abnormal temperature and velocity fields. When we prepare the user subroutine, the measures to prevent calculating any unrealistic viscosity-values are required. We expected the possible maximum and minimum values of viscosity and used the limits as cut off values. If maximum value exceeds twelve thousands, the original value is restricted to twelve thousands. The minimum value is one tenth. We could restrict the calculation results within the range of cut off values as the flow becomes to steady state. This method was helpful enough to obtain stable convergence of the solution.

4. Mixing performance index

Mixing is caused by shear deformation and elongation of polymer due to the complicated flow in screw extruder. Generally speaking, mixing is divided into two categories: a dispersive mixing and a distributive mixing. Dispersive mixing means at what degree the polymer particles are broken down into pieces, while distributive mixing means how far the neighboring particles' spatial distributions are. Dispersive mixing is meaningful only when the value is higher than yield point of some material and it always appears together with distributive mixing.

4.1. Dispersive mixing

A formula described in equation (6) is a definition of the magnitude of the rate-of-deformation tensor that can be used as a dispersive mixing index. In this study, we call it as the deformation rate. In equation (6), the first three terms express the elongation rate that measures how far the polymer melt particle is extended, while the last three terms represent the pure shear rate that measures how much the polymer melt particle is sheared.

$$|\dot{\gamma}(t)| = \left[\begin{array}{l} 2\left(\frac{\partial u}{\partial x}\right)^2 + 2\left(\frac{\partial v}{\partial y}\right)^2 + 2\left(\frac{\partial w}{\partial z}\right)^2 \\ + \left(\frac{\partial v}{\partial x} + \frac{\partial u}{\partial y}\right)^2 + \left(\frac{\partial w}{\partial y} + \frac{\partial v}{\partial z}\right)^2 + \left(\frac{\partial u}{\partial z} + \frac{\partial w}{\partial x}\right)^2 \end{array} \right]^{\frac{1}{2}} \tag{6}$$

4.2. Distributive mixing

Distributive mixing indices used in this study are a residence time distribution and a magnitude of strain. The residence time distribution shows the spatial distribution of polymer particles, especially the distribution in the axial direction. It is calculated by the particle tracking method based on the calculated velocity field. Particles are numerically traced by calculating the spatial distribution of particles that move according to the velocity field. Second order Runge-Kutta numerical integration scheme is used to track particles. We analyzed the residence time distribution by calculating particles' movements in the screw element as if massless particles are floated in the computed velocity

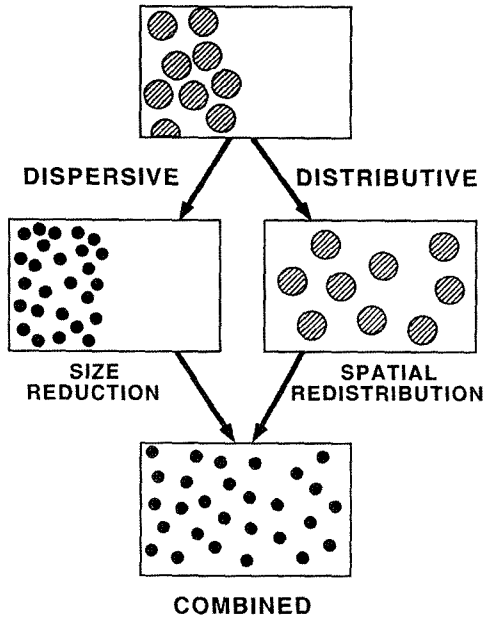

Fig. 5. Interrelationship between dispersive and distributive mixing.

field. To prevent the loss of particles due to flowing backward, all particles distribute evenly among all in front of the inlet cross section. The residence time distribution is indicated as a cumulated ratio of all tracking particles to particles that arrive at outlet. The value is expressed as a cumulative distribution function.

$$F(t) = C_{out}(t)/C_{\infty}, \tag{7}$$

where $C_{out}(t)$ is the number of particles that arrive in outlet according to time and C_{∞} is total number of tracking particles. Function $F(t)$ becomes zero when time t is zero and it becomes unity when time t approaches to infinite, while the slope of function cannot become negative. Another index of distributive mixing is a strain that is expressed in equation (8).

$$\gamma(t) = \int_0^t \dot{\gamma}(t)dt \tag{8}$$

The difference between the two indices is that the residence time distribution shows the characteristics of macroscopic mixing or bulk flow, while the strain shows the degree of microscopic mixing. That is to say, the residence time distribution represents a qualitative measure of distributive mixing, while the strain gives a quantitative one.

5. Results and discussion

5.1. Flow characteristics in screw extruder

The flow characteristics are investigated with the velocity field and the mass flux in the cross section of the screw extruder. All the results presented here are obtained in the

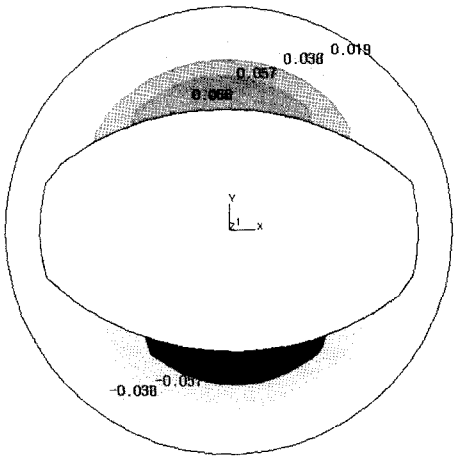

Fig. 6. Velocity [m/s] component u distribution in x-y plane [Pitch = 30 mm, rpm = 90].

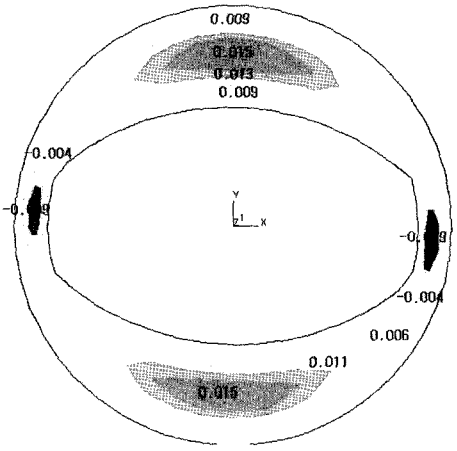

Fig. 7. Velocity [m/s] component w distribution in x-y plane [Pitch = 30 mm, rpm = 90].

middle cross section of the domain in the axial direction. The distribution of x-directional velocity component u is high near the screw surfaces and shows a symmetric distribution as shown in Fig. 6. The tendency is shown similarly in the distribution of y-directional velocity component v. The distribution of z-directional velocity component w is maximum at mid-height of channel as shown in Fig. 7. It is because that the flow resistance is low at mid-height of channel between the screw and barrel surfaces. Back flow is observed in the gap region where the distance between screw and barrel is minimum as shown in Fig. 11. This is resulted from the reverse direction of velocity gradient developed in the gap region as shown in Fig. 7.

The deformation rate is also high in the gap region as shown in Fig. 9. This has two meanings. One is that the effect of dispersive mixing is high in the gap region and the other is that the temperature in the gap region is high due to heat generation by the viscous dissipation as shown in

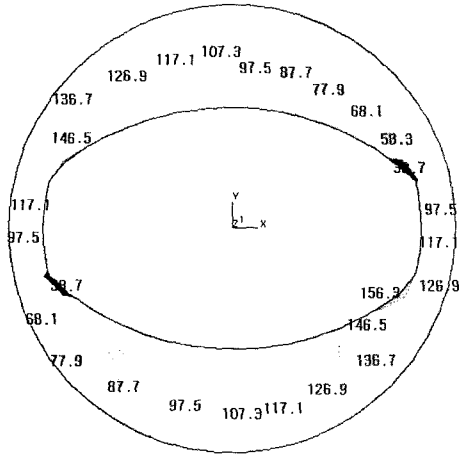

Fig. 8. Pressure [KPa] distribution in *x-y* plane [Pitch = 30 mm, rpm = 90].

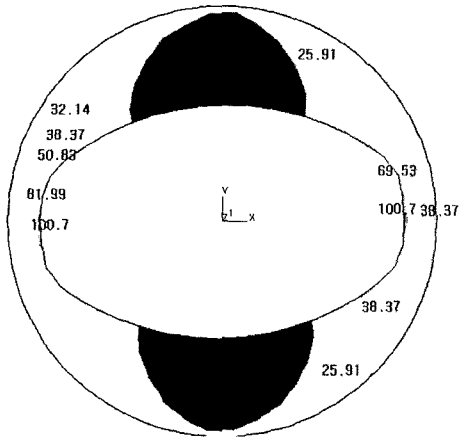

Fig. 9. Shear-rate [1/s] distribution in *x-y* plane [Pitch = 30 mm, rpm = 90].

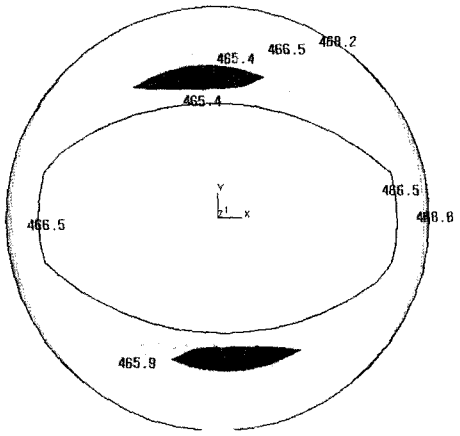

Fig. 10. Temperature [K] distribution in *x-y* plane [Pitch = 15 mm, rpm = 90].

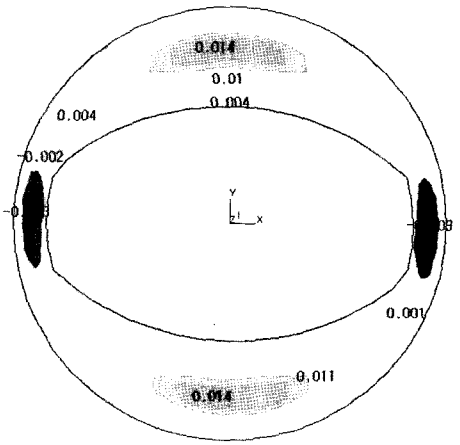

Fig. 11. Mass flux [g/s/mm^2] distribution in *x-y* plane [Pitch = 30 mm, rpm = 90].

Fig. 10. It has been identified that the viscosity is relatively low in the gap region where shear rate is higher than that of neighboring section. This is generally resulted from the typical shear thinning characteristic of polymer melt. Viscosity is high at low temperature region when the magnitude of shear rate is constant. This is resulted from the fact that the viscous model is a function of temperature and shear rate as mentioned in theory.

Pressure in the cross section rises in front of the gap region in the rotational direction and drops behind the gap region repeatedly as shown in Fig. 8. It is observed at the *x-y* cross section in detail that the pressure gradient changes in the gap region. This is resulted from the reduction of available space for the flow of polymer melt. Therefore, we can expect that the smaller gap region is, the higher pressure is. Mass flux as shown in Fig. 11 is also maximum at mid-height of channel like the distribution of velocity component *w*. In the gap region where the distance between barrel and screw is smaller, a back flow is observed due to the change of pressure gradient.

5.2. Flow and mixing characteristic with respect to parameters

The velocity component *u* in the *x*-direction in channel increases with the rise of screw speed and is high near the screw surface as shown in Fig. 12. The channel height means a maximum space distance between the screw surface and the barrel inner wall as shown in Fig. 2. The normalized height is defined as the distance from the surface of the screw element to the position of a material point in the channel. We can figure out that the velocity component *w* is influenced by both the screw rotation speed and the pitch length from the Fig. 13. That is to say, the larger the screw rotation speed and the pitch length are, the higher velocity component *w* is. The influence of the screw rotation speed and pitch length is also shown at mass flux sim-

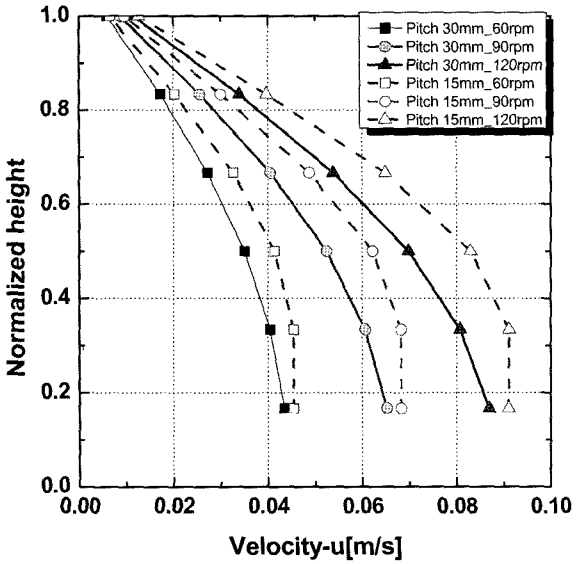

Fig. 12. Variation of velocity component u along the channel height.

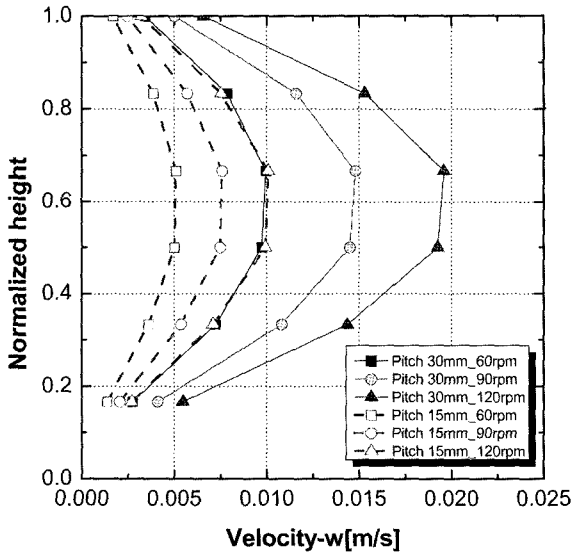

Fig. 13. Variation of velocity component w along the channel height.

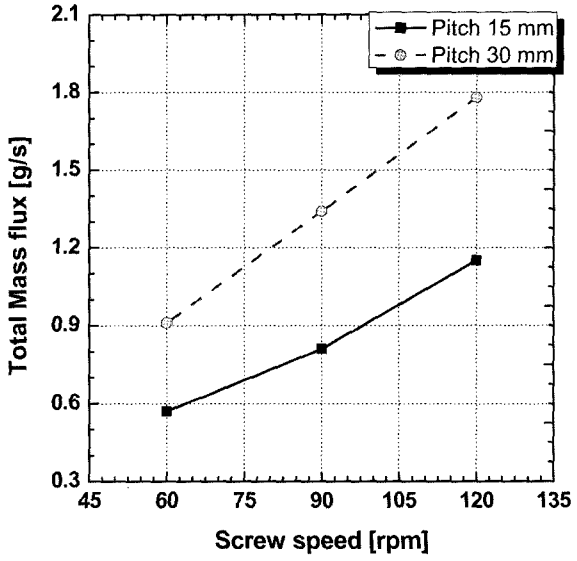

Fig. 14. Comparison of the total mass flux with respect to screw speed and screw pitch.

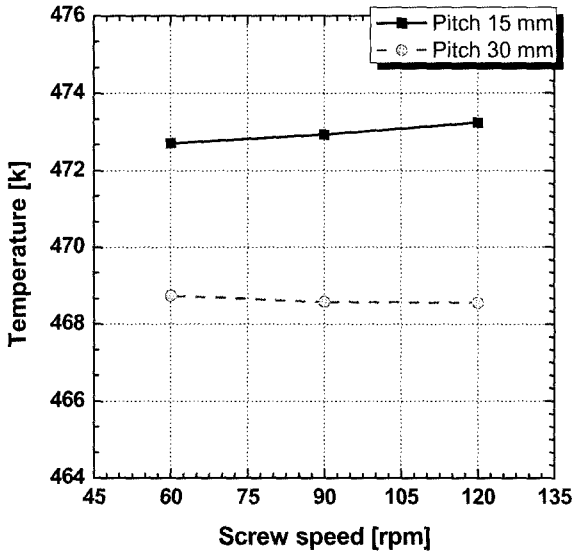

Fig. 15. Comparison of the temperature with respect to screw speed and screw pitch.

ilar to the velocity component w. That is to say, as shown in Fig. 14, the mass flux increases with the increment of screw rotation speed and pitch length due to the rise of velocity component w.

The average temperature at outlet is inversely proportional to pitch length but doesn't have the tendency to the increase of screw speed as shown in Fig. 15. The temperature influenced by the residence time and the deformation rate is higher due to the increase of residence time when the screw pitch is small. But the reason of temperature rise due to the increase of deformation rate is offset by the decrease of residence time when the screw speed is high. Fig. 16 shows the residence time of polymer melt using the average values of one hundred fifty particle points. As the screw rotation speed decreases and the pitch is smaller, the shift of curve to the right means the increase of residence time and being gentle of the curve slope means the rise of macro-mixing performance.

It is found that the deformation rate is proportional to the screw rotation speed, while there is little difference with respect the pitch length as shown in Fig. 17. So, the dispersive mixing performance is better when the screw speed is higher. Pure shear rate is higher with small

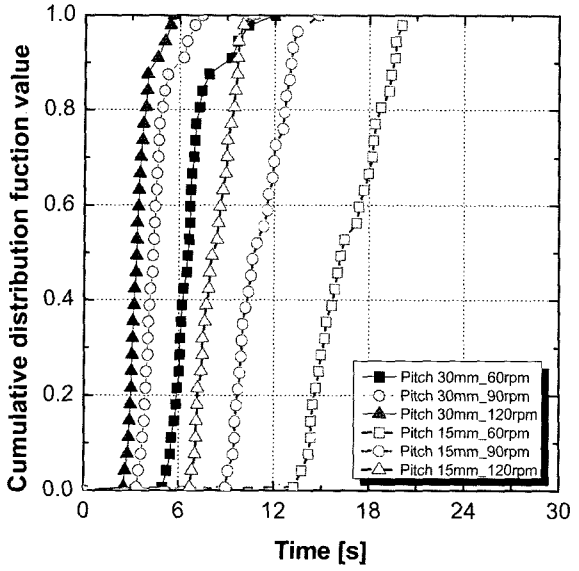

Fig. 16. Residence time obtained from the numerical tracers.

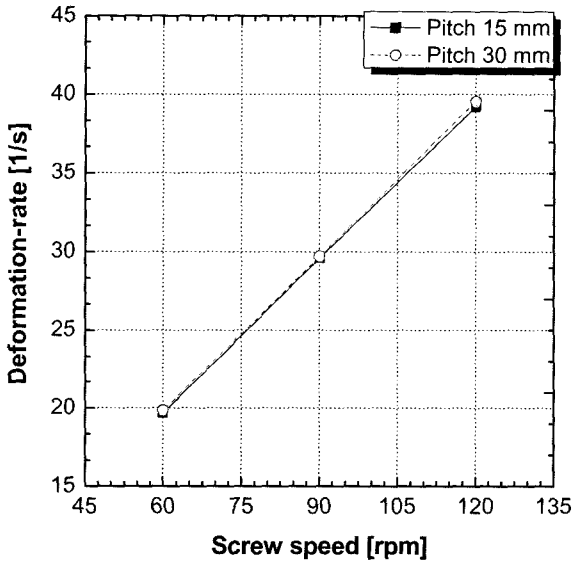

Fig. 17. Comparison of the deformation rate with respect to screw speed and screw pitch.

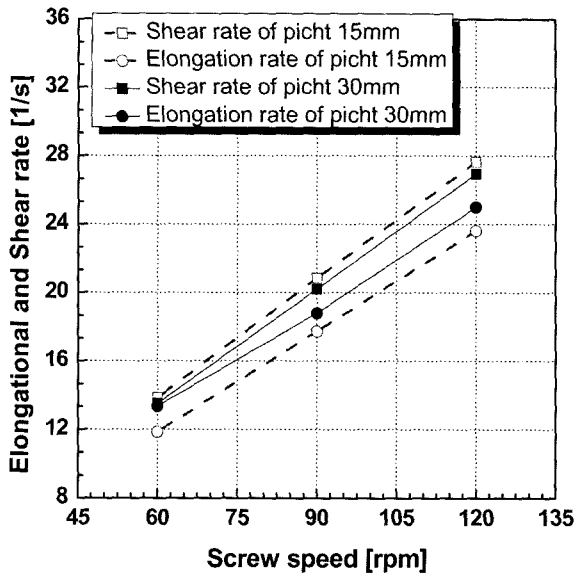

Fig. 18. Comparison of the elongation and shear rate with respect to screw speed and screw pitch.

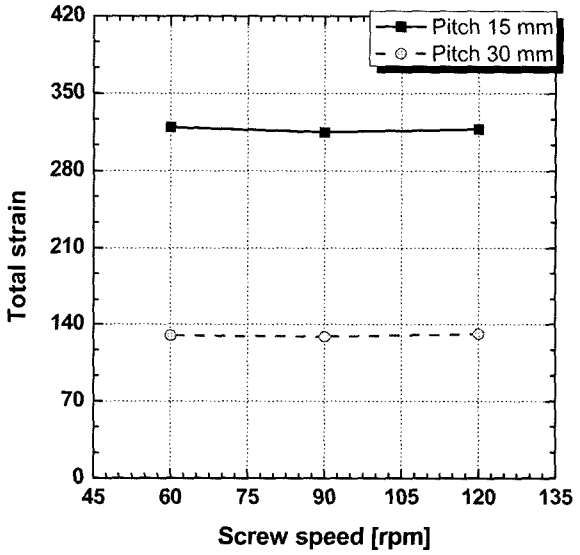

Fig. 19. Comparison of the strain with respect to screw speed and screw pitch.

screw pitch and the elongation rate becomes higher as the screw pitch is larger as shown in Fig. 18. It is reasoned that the gradient of velocity components u in Fig. 15 is bigger with the small screw pitch and the gradient of velocity components w in Fig. 13 is bigger with the larger screw pitch.

Total strain which is used as a distributive mixing index is shown in Fig. 19, according to the screw speed and the pitch. Each total strain is obtained by integrating the calculated deformation rate with respect to the residual time at each time increment. Generally, the total strain is proportional to the residence time and the deformation rate. So, it is observed when the screw pitch length is smaller the strain increases due to the increase of the residence time. But the strain doesn't show any tendency with the rise of screw rotation speed. It is regarded that the temperature rise due to the increase of deformation is offset by the reduction of residence time. Therefore it is not easy to generalize the fact that the mixing performance is proportional to the screw rotation speed, since the variations of the residence time and the deformation rate are dependent to the detailed shape of screw and barrel.

6. Conclusions

We calculated the velocity field around the metering section of screw element with varying the screw rotation speed that is an operation condition and the pitch length that is a shape parameter, with a commercial code, STAR-CD. The mixing performances are also analyzed in detail according to the parameters. The followings are concluded based on the computation results:

1. The velocity components u, v are high near the screw surface and the velocity component w is maximum at mid-height of channel.
2. The pressure is high in the gap region because available space for flow is small.
3. The high deformation rate in the gap region results in low viscosity together with high temperature due to much viscous dissipation.
4. As the screw rotation speed increases, both the mass flux and the deformation rate become higher, resulting in the better dispersive mixing performance.
5. As the screw length become small, the conveying capacity decreases, while the distributive mixing performance is better due to the increase of residence time of polymer melt.

Nomenclatures

$F_{h,j}$: diffusion energy flux in the x_j-direction
h_t : thermal enthalpy
n : power-law index
p : pressure
s_i : momentum source term
s_m : mass source term
$s_{c,m}$: rate of production or consumption of species m due to reaction
s_h : energy source term
T_{ref} : reference temperature
u_i : velocity components in the x_i-direction
u, v, w : velocity components in the x-, y-, z-directions respectively

Greek Letters

τ_{ij} : stress tensor components
ρ : mass density
δ_{ij} : Kronecker's delta
α : temperature shift factor
$\dot{\gamma}$: deformation rate
μ : viscosity
β : temperature sensitivity of μ
λ : a time constant
μ_0 : zero shear viscosity

Acknowledgements

This work was supported by Korean Research Foundation Grant (KRF-2004-005-D00001).

References

Ahmad, K. and C. Jean-Robert, 2005, Numerical simulation of non-isothermal three-dimensional flows in an extruder by a finite volume method, *J. non-Newtonian Fluid Mech.* **126**, 7.

Fenner, R.T., 1977, Development in the analysis of steady screw extrusion of polymers, *Polymer* **18**, 617.

Ghoreishy, M. and M.R. Nouri, 1999, Finite element analysis of thermoplastic melts flow through the metering and die regions of single screw extruder, *Inc. J. Appl. Polymer Sci.* **74**, 676.

Griffith, R.M., 1962, Fully developed flow in screw extruder, *Ind. Eng. Chem. Fundamentals* **1**, 180.

Karwe, M.V. and T. Jaluria, 1990, Numerical simulation of fluid flow and heat transfer in single screw extruder for non-Newtonian fluids, *Numerical*, Part A **17**, 167.

Kim, S.J. and T.H. Kwon, 1996a, Enhancement of mixing performance of single-screw extrusion processes via chaotic flows: Part 1, Basic concepts and experimental study, *Advances in Ploymer Tech.* **15**, 41.

Kim, S.J. and T.H. Kwon, 1996b, Enhancement of mixing performance of single-screw extrusion processes via chaotic flows: Part 1, Basic concepts and experimental study, *Advances in Ploymer Tech.* **15**, 41.

Kwag, D.S., W.S. Kim, K.S. Lee and M.Y. Lyu, 2001, A three-dimensional numerical study of fluid flow and heat transfer in the single screw extruder, *Proceeding of the second International Conference on Computational Heat and Mass Transfer*, 22-26.

Raman, V., Y. Chiruvella, Y. Jaluria and V. Sernas, 1996, Extrusion of non-newtonian fluid in a single-screw extruder with pressure back flow, *Polymer Eng. and Sci.* **36**, 358.

Sastrohartono, T., Y. Jaluria, M. Esseghir and V. Sernas, 1994, A numerical and experimental study of three-dimensional transport in the channel of an extruder for polymeric materials, *Int. J. Heat Mass Transfer* **38**, 1957.

Syrjala, S., 1999, On the analysis of fluid flow and heat transfer in the melt conveying section of a single screw extruder, *Numerical Heat Transfer*, Part A **35**, 25.

Syrjala, S., 2000, Numerical simulation of non-isothermal flow of polymer melt in a single screw extruder: A validation study, *Numerical Heat Transfer*, Part A **37**, 897.

Ye, Y.S., H.B. Kim, N. Kim and J.W. Lee, 2005, A study on analysis of polymer extruder process using the finite element method, *The Korean Society of Mechanical Engineers* Part A **29**, 145.